Stability of Mesoporous Oxide and Mixed Metal Oxide Materials under Biologically Relevant Conditions

John D. Bass, David Grosso, Cédric Boissiere, Emmanuel Belamie, Thibaud Coradin, and Clément Sanchez*

Chimie de la Matière Condensée, UMR UPMC-CNRS 7574, 4 place Jussieu, 75252 Paris 05, France

Received May 14, 2007. Revised Manuscript Received June 13, 2007

The dynamic behavior of nanoscale mesoporous oxide materials exposed to aqueous solutions under biologically relevant conditions is shown to be highly dependent on composition, porosity, and calcination temperature. Dynamic processes were followed as a function of exposure on thin oxide films amenable to environmental ellipsometry porosimetry for the analysis of mechanical strength and pore size distributions as a function of exposure. Additionally, X-ray photoelectron spectroscopy was used for the elucidation of compositional changes as a function of exposure. Combined, this approach gives the first detailed, quantitative information of the degradation of nanoscale oxide materials under biologically relevant conditions. This approach also shows the utility of using film geometry as a convenient model system for the study of dynamic properties, as films are amenable to sensitive ellipsometric characterization. Pure silica films underwent a rapid degradation, occurring on the time scale of hours, while silica films mixed with 10% or less of zirconia or alumina were significantly more stable. These mixed metal oxide films showed structural changes on two time scales, undergoing a rapid partial degradation followed by a stabilization of the structure as the composition of the films evolved toward a depleted silica state. The time scales of these two processes were on the order of hours and days, respectively, and could be tuned by varying the composition and the calcination temperature of the films. These time scales are especially relevant to the culture and growth of mammalian cells and for drug release applications. Titania materials were shown to be stable under all conditions studied, making them suitable candidates for applications where the scaffold functions as a permanent support. These results yield unprecedented levels of detail on the kinetics of degradation and the dynamic structural and compositional changes occurring in these nanostructured materials.

Introduction

The overlap between the materials and biology domains has opened an immense area for new fundamental research. Driving this research is the development of innovative systems, many bio-inspired or bio-mimetic,[1] for such applications as controlled drug release, advanced detectors, novel functional platforms for cancer therapy, and bioimaging.[2,3] These technologies fundamentally integrate and, in many cases, seek to control interactions between biological and synthetic components.

The ability to design effective interfaces between biological and synthetic materials will therefore have enormous impact on a range of problems, both in vivo, including bone repair/replacement materials and drug delivery vectors, and in vitro technologies, including biosensing, drug production, and environmental remediation.[4,5] In all cases, a critical design criterion, especially for materials with nanoscale features, is the dynamic behavior of the synthetic interface with respect to its operational environment. For some applications, the synthesis of a stable platform is preferred, as may be the case for building sensing devices with long operational lifetimes[6] or in the case of bone replacement devices.[7] In other cases, such as drug delivery and bone repair materials, the ability to construct tunable lifetimes is ideal, for the controlled release of biomolecules or as an avenue for controlling the residence time of bioabsorbable scaffolds.[8,9] Systems displaying transitional behaviors that lead to a final stable interface may also be advantageous, such as for the promotion of cell seeding on implantable devices.[10]

Compositional and textural control over properties on the nanoscale, including structure, mesoporosity, crystallinity, and wall thickness, are particularly interesting because their high surface area and ordered mesoporous structures make them attractive candidates for hosting bioactive compounds including proteins and drugs.[11] Much of the work to date on textured oxide bio-interfaces has been centered on the area of bone repair/replacement materials[12−16] and drug delivery

* Corresponding author. E-mail: clems@ccr.jussieu.fr.

(1) Sanchez, C.; Arribart, H.; Guille, M. M. G. *Nat. Mater.* **2005**, *4* (4), 277−288.
(2) Duguet, E.; Vasseur, S.; Mornet, S.; Devoisselle, J. M. *Nanomedicine* **2006**, *1* (2), 157−168
(3) Julián-López, B.; Boissière, C.; Chanéac, C.; Grosso, D.; Vasseur, S.; Miraux, S.; Duguet, E.; Sanchez, C. *J. Mater. Chem.* **2007**, *17*, 1563−1569.
(4) *Biomaterials Science*; Ratner, B. D., Hoffman, A. S., Schoen, F. J., Lemons J. E., Eds.; Academic Press: San Diego, 1996.
(5) Peppas, N. A.; Langer, R. *Science* **1994**, *263*, 1715−1720.
(6) Stenger, D. A; Gross, G. W.; Keefer, E. W.; Shaffer, K. M.; Andreadis, J. D.; Ma, W; Pancrazzio, J. J. *Trends Biotechnol.* **2001**, *19*, 304−309.
(7) Li, J. *Biomaterials* **1993**, *14*, 229−232.
(8) Malafaya, P. B.; Silva, G. A.; Baran, E. T.; Reis, R. L. *Curr. Opin. Solid State Mater. Sci.* **2002**, *6*, 283−295.
(9) Shin, H.; Jo, S.; Mikos, A. G. *Biomaterials* **2003**, *24*, 4353−4364.
(10) Hench, L. L.; Wilson, J. *Science* **1984**, *226*, 630−636.

10.1021/cm071305g CCC: $37.00
Published on Web 07/26/2007

Table 1. Summary of Textural Properties for Ordered Mesoporous Films upon Calcination

	material	SDA	calcination temperature	Young's modulus (GPa)	porosity	pore size[a] (nm)	surface area[b] (m^2/cm^3)
1	SiO_2	Pluronic F127	450 °C	6.9	31%	4.8/1.2	250
2	SiO_2	Pluronic F127	550 °C	8.6	28%	4.5/1.0	250
3	SiO_2	CTAB	450 °C	2.9	52%	2.8/1.4	500
4	$Si_{0.95}Zr_{0.05}O_2$	Pluronic F127	450 °C	6.0	44%	6.2/1.4	250
5	$Si_{0.95}Zr_{0.05}O_2$	Pluronic F127	550 °C	6.6	30%	6.8/1.3	230
6	$Si_{0.9}Zr_{0.1}O_2$	Pluronic F127	450 °C	6.1	41%	5.7/2.0	254
7	$Si_{0.9}Al_{0.1}O_x(OH_z)$	Pluronic F127	450 °C	4.1	28%	6.0/2.7	160
8	TiO_2	Pluronic F127	450 °C	4.1	36%	6.7/4.2	130

[a] Large axis tangential to the film surface/small axis of pore interconnections. [b] Geometric, based on the porosity and ellipsoidal pores in a cubic structure.

vectors.[11] In the former area, several groups have demonstrated, using titania,[12,16] bioactive glasses,[13−15,17−20] and mixed oxides,[21] that the composition and the textural properties are critical in determining the bioactivity of these materials. This dependence has been duplicated in cell culture studies on silica,[22] titania,[16] and alumina-based substrates,[23] where the nature of the interface was found to be critical in determining the attachment, growth, and morphology of cultured cells. In drug delivery systems, composition, pore size, and geometry are known to be critical for the design of controlled release delivery systems.[11]

Given the importance of compositional and textural properties on the observed response in biological systems and the potential to use such nanostructured materials for controlled delivery of biologically active agents, we set out to perform a detailed analysis of how such materials dynamically respond to their environment under biologically relevant conditions. Dynamic behavior can be predicted for such materials because the combination of high surface areas and low mass content that make them especially sensitive to interactions with their environment. Here, we focus on the use of thin, nanotextured oxide films as a model system to study, in detail, the dynamic nature of the interface.

The use of nanotextured oxide thin films as bio-inorganic interfaces has garnered recent attention as they provide a facile route for building controllable, biocompatible interfaces.[14−16,23] Furthermore, thin films provide a convenient geometry for the study of textural properties of nanoscale materials in general, being amenable to a variety of sensitive characterization tools, including X-ray photoelectron spectroscopy (XPS), transmission electron microscopy (TEM), and, more uniquely, ellipsometry. Analogous nanoscale materials can be readily synthesized as particles,[25] fibers,[25] or a variety of more complex morphologies.[26] In this work we examine how the textural properties of nanostructured films evolve under biologically relevant conditions, focusing on the use of environmental ellipsometry porosimetry (EEP) to yield detailed information on the porosity, pore structure, and dissolution behavior and XPS to yield information on compositional changes. Combined, this approach yields the first detailed, quantitative information on the degradation of nanostructured interfaces interacting with biological relevant environments.

Results and Discussion

Mesostructured thin films comprised of silica, silica−zirconia,[27] silica−alumina, and titania[28] were prepared by evaporation induced self-assembly[29] (EISA) using either amphiphilic triblock copolymers or ionic surfactants as structure directing agents (SDAs) yielding mesopores of 6 and 2 nm upon calcination, respectively. The effect of calcination on the stability of the film properties was carried out using two calcination temperatures, 450 °C and 550 °C. Thin films were exposed to aqueous environments at 37 °C consisting either of phosphate buffer solution (PBS) or cell culture media supplemented with 10% fetal bovine serum (FBS). Ellipsometry and EEP performed on calcined films before exposure, Table 1, reveal that the films are mesoporous with high specific surface areas and large pore volumes. Details on the film preparation, treatment, and characterization are given in Experimental Section.

For silica films, exposure to aqueous media has a marked effect on the textural properties as monitored by EEP. Figure 1 shows the observed index of refraction for silica film **1** as a function of the partial pressure of water upon exposure to PBS for 0, 25, and 60 min. At low humidity, the decrease in the index of refraction as a function of time is indicative of an increase in the pore volume in the film. Using a dense reference film prepared without a SDA to simulate the optical properties of the silica walls, the Bruggeman effective

(11) Vallet-Regi, M. *Chem.−Eur. J.* **2006**, *12*, 5934−5943.
(12) Cai, K.; Bossert, J.; Jandt, K. D. *Colloids Surf., B* **2006**, *49*, 136−144.
(13) López-Noriega, A.; Arcos, D.; Izquierdo-Barba, I.; Sakamoto, Y.; Terasaki, O.; Vallet-Regı, M. *Chem. Mater.* **2006**, *18*, 3137−3144.
(14) Yan, X.; Yu, C.; Zhou, X.; Tang, J.; Zhao, D. *Angew. Chem., Int. Ed.* **2004**, *43*, 5980−5984.
(15) Yan, X. X.; Deng, H. X.; Huang, X. H.; Lu, G. Q.; Qiao, S. Z.; Zhao, D. Y.; Yu, C. Z. *J. Non-Cryst. Solids* **2005**, *351*, 3209−3217.
(16) Zuruzi, A. S.; Butler, B. C.; MacDonald, N. C.; Safinya, C. R. *Nanotechnology* **2006**, *17*, 531−535.
(17) Vallet-Regi, M.; Ragel, C. V.; Salinas, A. J. *Eur. J. Inorg. Chem.* **2003**, 1029.
(18) Pereira, M. M.; Clark, A. E.; Hench, L. L. *J. Am. Ceram. Soc.* **1995**, *78*, 2463.
(19) Vallet-Regi, M.; Ramila, A. *Chem. Mater.* **2000**, *12*, 961.
(20) Vallet-Regi, M.; Arcos, D.; Perez-Pariente, J. *J. Biomed. Mater. Res.* **2000**, *51*, 23.
(21) Jokinen, M.; Pätsi, M.; Rahiala, H.; Peltola, T.; Ritala, M.; Rosenholm, J. B. *J. Biomed. Mater. Res.* **1998**, 295
(22) Zolkov, C.; Avnir, D.; Armon, R. *J. Mater. Chem.* **2004**, *14*, 2200−2205.
(23) Karlsson, M.; Pålsgård, E.; Wilshaw, P. R.; Di Silvio, L. *Biomaterials* **2003**, *24*, 3039−3046.
(24) Lu, Y. F.; Fan, H. Y.; Stump, A.; Ward, T. L.; Rieker, T.; Brinker, C. J. *Nature* **1999**, *398*, 223−226
(25) Bruinsma, P. J.; Kim, A. Y.; Liu, J.; Baskaran, S. *Chem. Mater.* **1997**, *9*, 2507−2512.
(26) Yang, H.; Coombs, N.; Ozin, G. A. *Nature* **1997**, *386*, 692−695.
(27) Soler-Illia, G. J. d. A. A.; Crepaldi, E. L.; Grosso, D.; Sanchez, C. *J. Mater. Chem.* **2004**, *14*, 1879.
(28) Grosso, D.; Soler-Illia, G. J. d. A. A.; Crepaldi, E. L.; Cagnol, F.; Sinturel, C.; Bourgeois, A.; Brunet-Bruneau, A,; Amenitsch, H.; Albouy, P. A.; Sanchez, C. *Chem. Mater.* **2003**, *15*, 4562−4570.
(29) Grosso, D.; Cagnol, F.; Soler-Illia, G. J. d. A. A.; Crepaldi, E. L.; Amenitsch, H.; Brunet-Bruneau, A.; Bourgeois, A.; Sanchez, C. *Adv. Funct. Mater.* **2004**, *14* (4), 309.

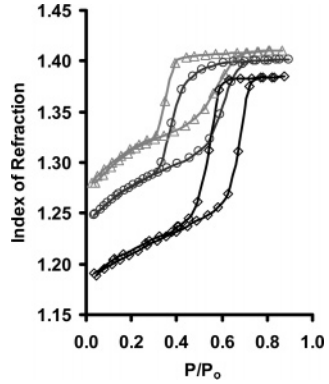

Figure 1. Water adsorption−desorption isotherms of a Pluronic templated silica film **1** as a function of exposure to PBS (pH 7.4) at 37 °C. Shown are data (△) before exposure, (○) after 25 min, and (◇) after 60 min. The index of refraction is given for $\lambda = 700$ nm.

medium approximation shows an increase in porosity from 30% to 65% upon 1 h of exposure, Figure 2. This increase in porosity, resulting from silica dissolution, decreases the Young's modulus of the film from ∼7 to below 1 GPa, Figure 2, as calculated from the thickness of the film upon reversible contraction caused by capillary stress.[30,31] After 90 min, the films no longer displayed sufficient mechanical stability to be measured using EEP. By ellipsometry, the film thickness remained homogeneous across the beam area (∼20 mm^2) even during dissolution.

The relative fraction of silica remaining in the film was determined from the porosity and film thickness, Figure 2. The observed rate of this decrease is well described by a simple reaction-limited dissolution model where dissolution is dependent only on the surface area, implying that the silica walls are homogeneous and there are no transport restrictions. Surface area measurements obtained using the porosity data and a geometric model describing the mesopore dimensions[30] (vida infra) allow for the extraction of a first-order rate constant, $k_1 = 2.7 \times 10^{-7}$ cm^3 silica/(m^2•s^1), describing the dissolution. Stability of silica films in Tris buffer at pH 7.3 was similar to that in PBS, yielding a first-order rate constant of 2.8×10^{-7} cm^3 silica/(m^2•s^1). This suggests that dissolution is not a consequence of the specific presence of phosphate but rather is pH-dependent (vida infra).

On the basis of the observed rate constants, the relative importance of internal transport restrictions under these conditions can be estimated by calculating the Thiele modulus. Assuming an effective diffusion coefficient of 2×10^{-8} cm^2 s^{-1},[32] transport restrictions would not be expected for films with thickness less than 80 μm. For spherical particles, transport restrictions would not be expected for diameters less than 500 μm. At smaller dimensions, such materials would be expected to follow the same kinetics observed in Figure 2, with ∼70% mass loss occurring in the first 2 h.

The first-order rate constant value were used to model the dissolution, Figure 2 (gray line), using values for the film thickness measured by ellipsometry and surface areas measured using EEP (the surface areas for the final two time points were estimated on the basis of the porosity because the low mechanical strength at these points does not allow for a direct measurement using EEP).

Silica titration using the blue silicomolybdic assay[33] was used to measure the quantity of silicic acid species in solution after dissolution. Films for these experiments were exposed to deionized water solutions to avoid interference from the buffer. After 1 week at 37 °C (final pH = 5), ellipsometric analysis indicates that 92% of the silica film was dissolved. By titration, this corresponds to the equivalent of 6.5 mmol silicate species per cm^3 in the calcined film. This gives a density of 0.4 g cm^{-3} assuming a stoichiometry of SiO_2, an underestimation given the large number of hydroxyl groups expected on this high surface area material and the fact that the titration is only sensitive to monomeric and dimeric silicic acid species.[33] Moreover, as a result of the selectivity of this measurement to monomeric and dimeric species, this assay indicates that dissolution results in the reduction of the film to molecular species.

EEP measurements were also used to observe changes in the pore size distribution as a function of time. In Figure 1, the steep increase in the refractive index due to filling of the mesopores by capillary condensation is seen to occur at higher partial pressures upon exposure. Pore size distributions for silica film **1**, Figure 3, were calculated using the isotropic inorganic pore contraction (IIC) model and the Kelvin equation modified for ellipsoidal pores.[30] Upon exposure, the absorption branch of the isotherm shows the radius of the mesopores increasing while desorption data show the opening of interconnections between pores. Given this behavior and the ability to describe the dissolution as a first-order rate process with respect to surface area, we suggest that dissolution occurs uniformly, gradually increasing the size of the pores and the porosity, decreasing the observed Young's modulus but without markedly affecting the film height or surface area, Figure 3 (inset).

Increasing the calcination temperature of the film decreases the rate of dissolution. For a film calcined to 550 °C the first-order rate constant for dissolution decreases by 40% to 1.6×10^{-7} cm^3 silica/(m^2•s^1) compared with film **1** calcined to 450 °C (2.7×10^{-7} cm^3 silica/(m^2•s^1)). The decrease in dissolution rate results from a higher degree of cross-linking caused by additional silica condensation. This also causes densification of the film, which contracts by 55% upon calcination to 550 °C as compared to 50% at 450 °C.

Exposure to cell culture media supplemented with 10% FBS resulted in somewhat faster degradation of the silica films, Figure 4. Silica film **1**, calcined to 450 °C, gave a first-order rate constant for dissolution of 5.0×10^{-7} cm^3 silica/(m^2•s^1). This increase in the dissolution rate is probably a result of the presence of active nucleophiles in the culture media, which greatly affect the chemical reactivity of silica species.[34]

(30) Boissiere, C.; Grosso, D.; Lepoutre, S.; Nicole, L.; Brunet Bruneau, A.; Sanchez, C. *Langmuir* **2005**, *21*, 12362−12371.
(31) Mogilnikov, K. P.; Baklanov, M. R. *Electrochem. Solid State Lett.* **2002**, *5*, F29.
(32) Etienne, M.; Quach, A.; Grosso, D.; Nicole, L.; Sanchez, C.; Walcarius, A. *Chem. Mater.* **2007**, *19*, 844.
(33) Coradin, T.; Eglin, D.; Livage, J. *Spectroscopy: Int. J.* **2004**, *18*, 567−576.
(34) *Ultrastructure Processing of Advanced Ceramics*; Corriu, R. J. P., Leclercq, D., Vioux, A., Pauthe, M., Phalippou, J., Mackenzie, J. D., Ulrich, D. R., Eds.; Wiley: New York, 1988, p 113.

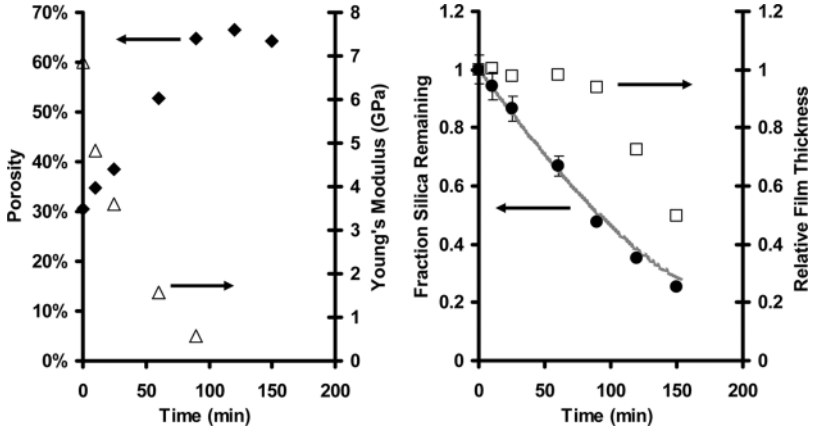

Figure 2. (Left) Porosity and Young's modulus of silica film **1** and (right) the fraction silica remaining in the film and the relative thickness of the film as a function of exposure to PBS at 37 °C.

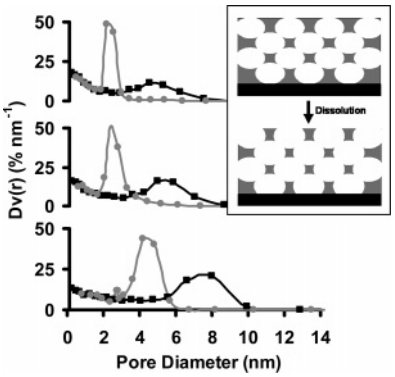

Figure 3. Pore size distribution of silica film **1** determined using EEP (top) before exposure and upon exposure to PBS for (middle) 25 min and (bottom) 60 min. The adsorption branch (■) shows how the pore size distribution increases. The desorption branch (●) shows how the pore interconnections open over time. Inset: Dissolution occurs uniformly as a first-order process with respect to surface area, gradually increasing the size of the pores and the porosity, decreasing the observed Young's modulus but without markedly affecting the film height or surface area.

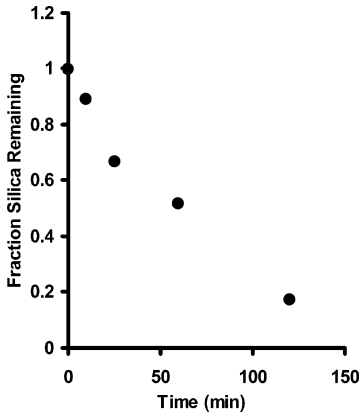

Figure 4. Fraction of silica remaining in silica film **1** as a function of exposure to cell culture media supplemented with 10% FBS at 37 °C.

Silica films templated with cetyltrimethylammonium bromide (CTAB) were also highly hydrolytically unstable. Indeed, when calcined to 450 °C, they showed ~70% dissolution in the first 2 h, yielding an initial rate constant for dissolution of 1.0×10^{-7} cm^3 silica/(m^2•s^1). This value is very sensitive to the measured surface area and is therefore probably underestimated by using a geometric surface area measurement, as observed in previous work for CTAB films.[30] This value is comparable to the pluronic films, Table 2, perhaps because the higher surface area from mesopores is offset to the greater microporosity observed in pluronic templated films caused by interpenetration of poly(ethylene oxide) chains in the silica matrix.[35]

Kinetic experiments were also conducted on particle geometry using SBA-15 mesoporous silica.[36,37] Rapid silica dissolution was also observed in this system, as monitored by the silicomolybdic assay. The time scale for dissolution in this material was slightly longer, achieving 60% overall dissolution in 5 h. The slightly slower kinetics can be attributed to synthesis at 130 °C, conditions specifically chosen to minimize microporosity for the creation of dense silica walls.[36] As in the case of films presented here, these kinetics should be tunable on the basis of the calcination procedure, the use of specific templating agents (CTAB, Pluronic, etc.) for the creation of different mesoporous morphologies (MCM, MSU, etc.), and the inclusion of other nonsilica metal centers (vida infra).

One method for the tuning of nanotextured oxides is the creation of mixed metal oxides through the incorporation of metal centers with different chemical characteristics at various compositional ranges.[27] With this in mind, we synthesized silica rich silica−zirconia[27] and silica−alumina films to investigate the dynamic behavior of these films under biologically relevant conditions.

As prepared, silica−zirconia films have slightly higher porosity and larger pores compared with pure silica films. EEP results for silica−zirconia films upon exposure to PBS at 37 °C show that these films are much more hydrolytically stable, with dynamic behaviors that are more complex than pure silica films. This is consistent with results showing an increased stability for mesoporous silica materials under hydrothermal conditions upon the incorporation of metallic heteroatoms (Al, Ti, etc.).[38−40] The sorption behavior of water in a 5% zirconia film **4** calcined to 450 °C is shown in Figure

(35) Melosh, N. A.; Lipic, P.; Bates, F. S.; Wudl, F.; Stucky, G. D.; Fredrickson, G. H.; Chmalka, B. F. *Macromolecules* **1999**, *32*, 4332.
(36) Galarneau, A.; Cambon, H.; Di Renzo, F.; Fajula, F. *Langmuir* **2001**, *17*, 8328−8335.
(37) Zhao, D. Y; Feng, J. L.; Huo, Q. S.; Melosh, N.; Fredrickson, G. H.; Chmelka, B. F.; Stucky, G. D. *Science* **1998**, *279* (5350), 548−552.
(38) Chen, L. Y.; Jaenicke, S.; Chuah, G. K. *Microporous Mater.* **1997**, *12*, 323.
(39) Shen, S.-C.; Kawi, S. *J. Phys. Chem. B* **1999**, *103*, 8870−8876.
(40) Han, Y.; Li, N.; Zhao, L.; Li, D.; Xu, X.; Wu, S.; Di, Y.; Li, C.; Zou, Y.; Yu, Y.; Xiao, F.-S. *J. Phys. Chem. B* **2003**, *107*, 7551−7556.

Table 2. Initial Dissolution Rates of Textured Oxide Materials

	material	SDA	calcination temperature	k_{ini}: PBS, cm^3 silica/(m^2·s)	k_{ini}: cell culture media, cm^3 silica/(m^2·s)
1	SiO_2	Pluronic F127	450 °C	2.7×10^{-7}	5.0×10^{-7}
2	SiO_2	Pluronic F127	550 °C	1.6×10^{-7}	
3	SiO_2	CTAB	450 °C	1.5×10^{-7}	
4	$Si_{0.95}Zr_{0.05}O_2$	Pluronic F127	450 °C	4.7×10^{-8}	6.0×10^{-8}
5	$Si_{0.95}Zr_{0.05}O_2$	Pluronic F127	550 °C	1.3×10^{-8}	
6	$Si_{0.9}Zr_{0.1}O_2$	Pluronic F127	450 °C	2.4×10^{-9}	
7	$Si_{0.9}Al_{0.1}O_x(OH_z)$	Pluronic F127	450 °C	8.8×10^{-9}	
8	TiO_2	Pluronic F127	450 °C	~0	

5 at 0, 4, and 48 h of exposure. During the first 8 h, the refractive index at low humidity decreases significantly and the observed Young's modulus calculated from EEP decreases from 6 to 3 GPa, indicating an increase in the porous volume of the film, Figure 6. At early times, an initial rate constant for dissolution was measured to be 4.7×10^{-8} cm^3 silica/(m^2·s^1), about 6 times slower than its pure silica counterpart. At longer times, the sorption behavior of the films changes much more slowly with respect to exposure while the relative thickness of the film remains essentially constant, decreasing by only 5% over 72 h, Figure 6. Zirconia films in cell culture media supplemented with 10% FBS showed similar rates of dissolution as those in PBS, giving 6×10^{-8} cm^3 silica/(m^2·s^1) for 5% zirconia. Silica−zirconia films at 10% zirconia (film **6**) are even more stable, giving an initial rate constant for dissolution of 2.4×10^{-9} cm^3 silica/(m^2·s^1), or 100 lower than that of a pure silica film exposed to PBS.

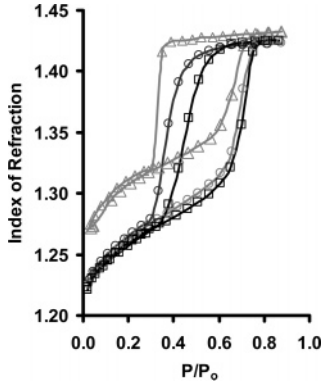

Figure 5. Water adsorption−desorption isotherms of a Pluronic templated silica−zirconia film **4** as a function of exposure to PBS (pH 7.4) at 37 °C. Shown are data (△) before exposure, (○) after 4 h, and (□) after 48 h. The index of refraction is given for $\lambda = 700$ nm.

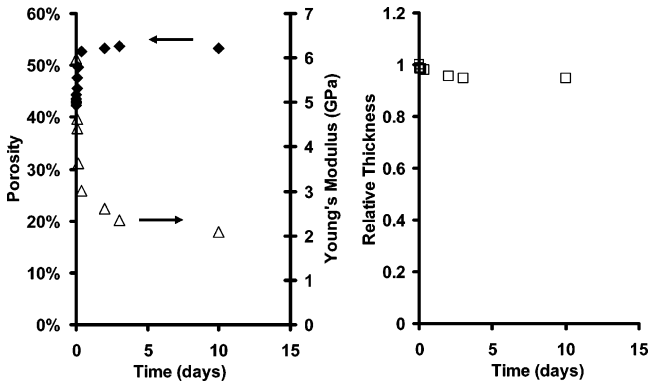

Figure 6. (Left) Porosity and Young's modulus of silica−zirconia film **4** as a function of exposure to PBS at 37 °C. Porosity measurements assume that the refractive index of the walls remains unchanged, resulting in a likely underestimation the porosity at longer times. (Right) The relative thickness as a function of exposure time demonstrates the increased stability of these films over pure silica films.

The behavior of the film can be explained by an initial loss of silica resulting in a film with increasing zirconia content and consequently an even more hydrolytically stable structure. By XPS analysis, the ratio of zirconia to silica is seen to increase in the film **4** from 0.045:1 before exposure to 0.076:1 after 11 days. Similar increases are seen in the silica zirconia system with higher zirconia content. The dissolution behavior is not a consequence of saturation in the media because replacement with fresh media after films have stabilized has no effect. Had saturation of the solution with silicate caused the stabilization of the film via equilibration, replacement of the media would have led to additional film mass loss and the establishment of a new equilibrated state. Given the increasing zirconia content of the films, the porosity values calculated from ellipsometry are underestimated (~5−10%) by a small extent at longer times, as a result of the assumption that the refractive index of the walls remains constant.

XPS analysis also shows an uptake of phosphorus, originating from the buffer, upon exposure. After 11 days in the low zirconia system, **4**, the ratio of zirconia to phosphorus species is 1 to 1.2. Likewise, a zirconia to phosphorus ratio of 1 to 1.3 is observed in the high zirconia content system, **6**, after 20 h of exposure. This behavior is expected given the strong complexation that can occur between phosphate species and zirconia.[41] The scaling of phosphate with zirconia content is interesting from the standpoint of drug delivery in that it provides the opportunity to tailor the controlled capture and release of bioactive molecules on the basis of metal complexation.[42]

The pore size distribution for zirconia film **4** was calculated from EEP data as shown in Figure 7 (measurements that are unaffected by changes in the refractive index of the inorganic matrix). The increased hydrolytic stability with respect to pure silica films is again observed, with a slower opening of the pore structure. After 72 h, the large axis of the pores increases from 6.5 to 7.8 nm while the interconnections increase in size from 2.9 to 4.5 nm. The slightly larger effect seen for the interconnections is most likely due to their convex structure, which imparts a higher curvature and thus would be expected to reduce the stability in these regions.

Changes in silica−zirconia films are seen to occur over two time scales, an initial sharp increase in porosity and

(41) Angelomé, P. C.; Aldabe-Bilmes, S.; Calvo, M. E.; Crepaldi, E. L.; Grosso, D.; Sanchez, C.; Soler-Illia, G. J. d. A. A. *New J. Chem.* **2005**, *29*, 59−63.
(42) Angelomé, P. C.; Soler-Illia, G. J. d. A. A. *Chem. Mater.* **2005**, *17*, 322−331.

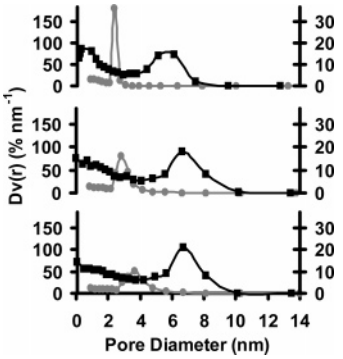

Figure 7. Pore size distribution of 5% zirconia film **4** determined using EEP (top) before exposure and upon exposure to PBS for (middle) 8 h and (bottom) 48 h. The adsorption branch, right axis (■), shows how the pore size distribution of the large axis tangential to the film surface, increases. The desorption branch, left axis (●), shows how the bottlenecks between pores open over time.

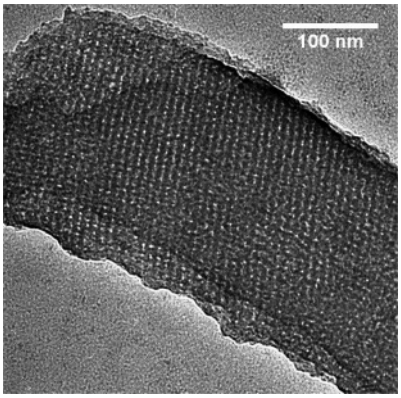

Figure 8. TEM image of silica−alumina film **7** templated with pluronic after calcination.

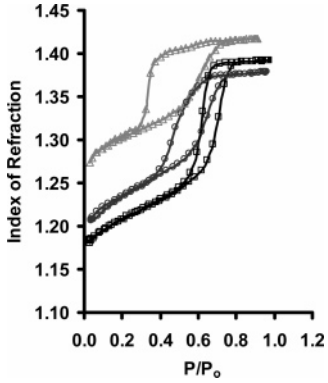

Figure 9. Water adsorption−desorption isotherms of a Pluronic templated silica−alumina film **7** as a function of exposure to PBS (pH 7.4) at 37 °C. Shown are data (△) before exposure, (○) after 21 h, and (□) after 65 h. The index of refraction is given for $\lambda = 700$ nm.

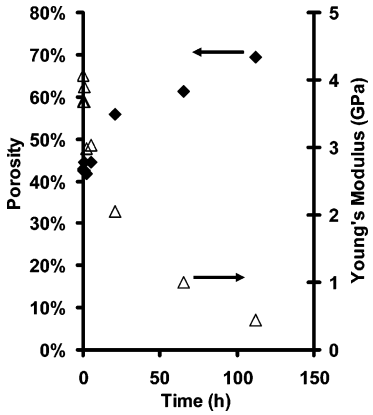

Figure 10. Porosity and Young's modulus of silica−alumina film **7** as a function of exposure to PBS at 37 °C.

reduction in stiffness over the first several hours followed by more subtle changes in pore structure, mainly seen in an opening of the restrictions between pores, occurring on the time scale of days. Both of these time scales are biologically relevant, with the former covering the attachment and spreading of mammalian cells during culture, and the latter on the time scale of mammalian cell growth and division.[43] These time scales can be tuned by varying the calcination temperature or the zirconia content of the films. Increasing the calcination temperature to 550 °C decreases the initial rate of dissolution by ∼75% to a value of 1.3×10^{-8} cm^3 silica/(m^2•s^1). Increasing the zirconia content has a similar stabilizing effect on the films (see above).

As prepared, silica−alumina (10% Al) films have similar porosity as compared with pure silica films, although with a larger average pore size and a decrease in the surface area and Young's modulus. TEM analysis of silica−alumina materials, Figure 8, shows the ordered nature of the films after calcination. The sorption behavior of water in a silica−alumina film calcined to 450 °C is shown in Figure 9 at 0, 21, and 65 h of exposure. EEP results for silica−alumina films upon exposure to PBS at 37 °C show that these films are also much more hydrolytically stable than pure silica films, Figure 10, but less stable than the silica−zirconia films at similar substitution levels. At early times, an initial rate constant for dissolution was measured to be 8.8×10^{-9} cm^3 silica/(m^2•s^1), about 30 times slower than the pure silica counterpart. Similar to silica−zirconia films, silica−alumina films show two dissolution behaviors, an initial loss of mass followed by a more gradual decrease at longer times. Also similar to the silica−zirconia system, the pore interconnections appear to demonstrate decreased stability as compared to the overall structure. This again can be ascribed to the convex nature of these structures.

By XPS analysis the alumina to silica ratio is seen to increase slightly from 0.12:1 before exposure to 0.16:1 after 20 h. Unlike in the silica−zirconia system, the increasing alumina content of the films has minimal impact on the calculated porosity, Figure 11, in this system because the index of refraction is not strongly dependent on alumina substitution. XPS analysis shows virtually no uptake of phosphorus species, with a ratio of silica to phosphorus of 1 to 0.006 after 20 h.

Finally, we studied the behavior of mesoporous titania films[28] upon exposure to aqueous media at 37 °C. Titania films have received much attention as bio-inorganic interfaces as titanium, and titanium alloys are frequently used in biomaterial applications.[12,16]

Titania films were highly porous with a larger average pore size comparable to the silica−alumina materials. The surface area and Young's modulus were also similar to the silica−alumina materials. EEP results upon exposure to PBS at 37 °C show these films to be extremely hydrolytically stable compared with the other films studied. Data were

(43) Anselme, K.; Bigerelle, M. *Biomaterials* **2006**, *27*, 1187−1199.

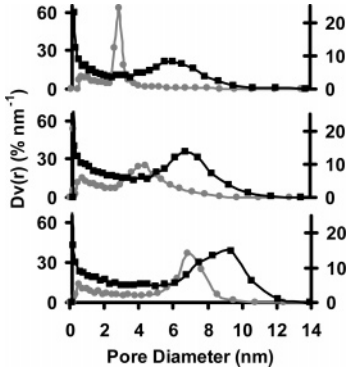

Figure 11. Pore size distribution of silica−alumina film **7** determined using EEP (top) before exposure, (middle) upon exposure to PBS for 8 h, and (bottom) upon exposure for 48 h. The adsorption branch, right axis (■), shows how the pore size distribution of the large axis tangential to the film surface, increases. The desorption branch, left axis (●), shows how the bottlenecks between pores open over time.

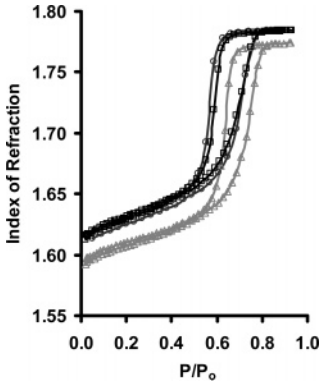

Figure 12. Water adsorption−desorption isotherms of a Pluronic templated titania film **8** as a function of exposure to PBS (pH 7.4) at 37 °C. Shown are data (△) before exposure, (○) after 4 h, and (□) after 24 h. The index of refraction is given for $\lambda = 700$ nm.

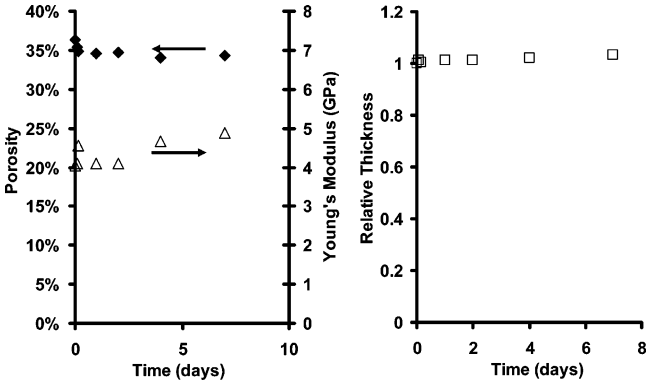

Figure 13. (Left) Porosity and Young's modulus of titania film **8** as a function of exposure to PBS at 37 °C. (Right) The relative thickness as a function of exposure time shows that the film remains relatively unchanged.

collected using PBS solutions, because significant protein absorption present with cell culture media supplemented with FBS prevented an accurate quantitative description of the film behavior.

The sorption behavior of water in a titania film calcined to 450 °C is shown in Figure 12 at 0, 4, and 24 h of exposure. No titania loss could be detected in the system after more than 1 week. The porosity, Young's modulus, and relative thickness remain relatively constant, Figure 13, as well as the pore size distribution, Figure 14. The initial small decrease in the porosity (Figure 13) and the slight decrease

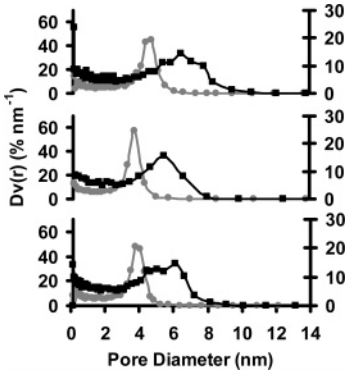

Figure 14. Pore size distribution of titania film **8** determined using EEP (top) before exposure and upon exposure to PBS for (middle) 4 h and (bottom) 24 h. The adsorption branch, right axis (■), shows the pore size distribution of the large axis tangential to the film surface. The desorption branch, left axis (●), shows the bottlenecks between pores.

in the observed pore size distribution (Figure 14) are believed to be due to the adsorption of phosphate onto the titania surface.[44,45] This is corroborated by XPS analysis that shows a ratio of 0.14 phosphorus species per titania after 7 days of exposure, although an increase in surface hydroxylation may also contribute to the pore constriction and the corresponding decrease in porosity. Such phosphate absorption is again interesting from the standpoint of drug delivery in that it provides the opportunity to tailor the controlled capture and release of bioactive molecules on the basis of metal complexation.[42]

Conclusions

Mesoporous oxide materials including particles and thin films exposed to aqueous environments under biologically relevant conditions display a range of dynamic behaviors dependent on their composition, porosity, and calcination temperature. The time scale of these dynamic behaviors, ranging from hours to days, is especially relevant to the culture and growth of mammalian cells and to the use of these materials for drug release applications. The complete degradation of silica films, for example, occurs over the same time scale as the attachment and spreading of many types of mammalian cells, and the near constant degradation rate as a function of time makes these potentially interesting materials for the uniform release of bioactive molecules over similar time scales. Similar dissolution kinetics are seen using SBA-15 silica particles, whose geometry can be envisioned for applications as drug release vectors. Both of these silica systems result in dissolution down to molecular species. In contrast to pure silica systems, silica−zirconia and silica−alumina films show structural changes on both a short time scale and a longer time scale more relevant to the growth and division of mammalian cells. This hybrid behavior combines the transitional properties of silica films with the structural integrity demonstrated by titania films. Such structural integrity is important for applications where the

(44) Brown, G. E.; Henrich, V. E.; Casey, W. H.; Clark, D. L.; Eggleston, C.; Felmy, A.; Goodman, D. W.; Gratzel, M.; Maciel, G.; McCarthy, M. I.; Nealson, K. H.; Sverjensky, D. A.; Toney, M. F.; Zachara, J. M. *Chem. Rev.* **1999**, *99*, 77−174.
(45) Nooney, M. G.; Campbell, A.; Murrell, T. S.; Lin, X. F.; Hossner, L. R.; Chusuei, C. C.; Goodman, D. W. *Langmuir* **1998**, *14*, 2750−2755.

scaffold functions as a permanent support. Furthermore, the ability to control the dissolution process via the calcination temperature and composition provides a convenient route to tailor the interface for tunable lifetime applications. From the standpoint of drug delivery, the scaling of bound phosphate as a function of both metal content and type is interesting in that it provides the opportunity to tailor the controlled capture and release of bioactive molecules based on metal complexation. Finally, this work demonstrates that the use of film geometry, which is amenable to sensitive characterization techniques such as ellipsometry, can serve as an excellent platform for the study of dynamic processes in nanomaterials. This approach has important repercussions for many advanced applications, including applied fields at the intersection of materials and biology.

Experimental Section

All products were purchased from Sigma/Aldrich and used as furnished. Oxide films were prepared, as reported previously, in the presence of CTAB or F127 Pluronic block copolymer as structuring agents by dip-coating.[24,29] Dense films were prepared in the same manner but in the absence of the SDA. Silica films were prepared from solutions of molar ratios 1:35:5:0.08:0.14 TEOS/EtOH/H_2O/HCl/CTAB (or 0.004 F127), which were aged at room temperature for 3 days. Films were prepared on silicon substrates using a withdrawal rate of 1.6 mm s^{-1} (dense films at 2.7 mm s^{-1}) under 30% relative humidity (RH). After the dry line reached the bottom of the film, the RH was immediately increased to 70% and held for 5 min. Titania films were prepared from fresh solutions, molar ratios 1:40:15:0.004 $TiCl_4$/EtOH/H_2O/F127, using a withdrawal rate of 0.9 mm s^{-1} at a RH less than 15%. The RH was increased to 75%, and films were held for 1 min upon the termination of the dry line. Silica−zirconia films were prepared from fresh solutions, with the molar ratio 0.9:0.1:40:10:0.005 TEOS/$ZrCl_4$/EtOH/H_2O/F127 (for 10% Zr), using a withdrawal rate of 1.6 mm s^{-1} (dense films at 2.7 mm s^{-1}) at a RH less than 10%. Templated films were subsequently exposed to saturated water vapor for 5 s. Silica−alumina films were prepared from fresh solutions, with the molar ratio 0.9:0.1:40:10:0.005 TEOS/$AlCl_3$·$6H_2O$/EtOH/H_2O/F127, using a withdrawal rate of 1.6 mm s^{-1} (dense films at 2.7 mm s^{-1}) at a RH less than 10%. Templated films were subsequently exposed to saturated water vapor for 20 s. After coating, silica and titania films were aged in a 75% RH environment overnight and subsequently cured at 130 °C for 24 h. Silica−zirconia and silica−alumina films were held in a 50% and 70% RH environment, respectively, overnight before being transitioned to a 60 °C oven for 8−10 h and further cured at 130 °C for 24 h. Calcination was carried out in air using a 5 °C/min ramp rate with the films held at the desired final temperature for 10 min. Removal of organic residues by calcination led to ordered mesoporous films with monodispersed pores. Ellipsometry measurements were performed on a UV−visible (from 240 to 1000 nm) variable angle spectroscopic ellipsometer (VASE) from Woollam, and the data analysis was performed with the WVase32 software. For environmental porosimetry measurements the ellipsometer was fitted with a small, variable humidity flow chamber flushed with 2.5 L of air/min. The humidity was adjusted using a mass flow controller and monitored using a RH probe held in the environmental chamber.[30]

Films, approximately 2 cm^2, were exposed to 8 mL of either PBS (pH 7.4 at 25 °C), Tris (100 mM 2-Amino-2-(hydroxymethyl)-1,3-propanediol adjusted to pH 7.6 at 25 °C with HCl), or Dulbecco's modified Eagle's medium supplemented with 10% FBS (also containing penicillin/streptomycin and fungicide) at 37 °C. PBS solution was prepared from 10X stock solutions and contained 8 mM sodium phosphate, 0.8% NaCl, and 0.02% KCl. It did not contain any Ca^{2+}, Mg^{2+}, and so forth that might otherwise have complicated the analysis. For testing, films were removed and washed with a minimum amount of distilled water, ∼1 mL, and dried under nitrogen flow. Ellipsometry was conducted at room temperature (25 °C) under a constant 2.5 L/min flux of air with a controlled water partial pressure. EEP was conducted using the adsorption−desorption isotherm of water analyzed with an isotropic inorganic pore contraction model (IIC) and a modified Kelvin equation for ellipsoidal pores.[30]

Silica titration was carried out using silica substrates polished on both sides. A 2 cm^2 section was prepared from a larger film by removal of the bottom and sides (where the film thickness may be expected to vary). Films were added with 5 mL of deionized water and left at 37 °C for 1 week. The film was evaluated using ellipsometry, and the solution titrated using the blue silicomolybdic assay according to published procedures[33] on a Uvikon UV−vis spectrophotometer using an extinction coefficient of 44 700 M^{-1} cm^{-1} at 810 nm. This procedure was also used to follow the dissolution of SBA-15 mesoporous silica particles synthesized (at 130 °C) according to ref 36 (∼2 mg, 8 nm pore diameter, ∼650 m^2 g^{-1}) suspended in PBS (50 mL) at 37 °C. For this experiment the silica to solution ratio was approximately 10 times higher than in the film based experiments.

Surface chemical compositions were analyzed by XPS (ESCALAB 250, Al Kα (1486.6 eV) source, take-off angle = 90°). TEM micrographs were collected using a Philips CM12 transmission microscope. Samples were obtained by scratching the films from the substrate and depositing them on coated copper grids.

Acknowledgment. J.D.B. is grateful to the National Science Foundation for an International Research Fellowship. The authors acknowledge funding provided by CNRS and UPMC.

CM071305G